

Explaining 95 (or so) GeV Anomalies in the 2-Higgs Doublet Model Type-I

AKSHAT KHANNA,^{1,*} STEFANO MORETTI,^{2,3,†} and AGNIVO SARKAR^{4,‡}

¹*Department of Physics, Indian Institute of Technology Gandhinagar, Gujarat 382055, India.*

²*School of Physics & Astronomy, University of Southampton, Highfield, Southampton SO17 1BJ, UK.*

³*Department of Physics & Astronomy, Uppsala University, Box 516, 75120 Uppsala, Sweden.*

⁴*Regional Centre for Accelerator-based Particle Physics, Harish-Chandra Research Institute, HBNI, Chhatnag Road, Jhansi, Prayagraj (Allahabad) 211019, India*

We show how the 2-Higgs Doublet Model (2HDM) Type-I can explain some excesses recently seen at the Large Hadron Collider (LHC) in $\gamma\gamma$ and $\tau^+\tau^-$ final states in turn matching Large Electron Positron (LEP) data in $b\bar{b}$ signatures, all anomalies residing over the 90-100 GeV or so region. The explanation to such anomalous data is found in the aforementioned scenario when in inverted mass hierarchy, in two configurations: i) when the lightest CP-even Higgs state is alone capable of reproducing the excesses; ii) when a combination of such a state and the CP-odd Higgs boson is able to do so. To test further this scenario, we present some Benchmark Points (BPs) of it amenable to phenomenological investigation.

I. INTRODUCTION

A long-standing anomaly existing in LEP collider data [1] is the one hinting at the possibility of $e^+e^- \rightarrow Zh$ events being produced therein, with a Higgs boson state h with a mass of approximately 98 GeV decaying into $b\bar{b}$ pairs [2]. More recently, the CMS collaboration at the LHC has found an excess near 95 GeV in di-photon events in two separate analyses [3, 4]. In fact, they also reported an excess in $\tau^+\tau^-$ pairs, again, around a mass of about 98 GeV. Finally, ATLAS also observed an excess at around 95 GeV in di-photon events, thereby aligning with CMS although, especially when including ‘look elsewhere’ effects, their findings are far less significant than the CMS ones. Altogether, in view of the limited mass resolution of the di-jet invariant mass at LEP, this older anomaly may well be consistent with the excesses seen by CMS (and, partially) ATLAS in the $\gamma\gamma$ and, even more so, $\tau^+\tau^-$ final states (as the mass resolution herein is also rather poor).

As a consequence of this credible mass overlap, many studies [5–35] have tested the possibility of simultaneously fitting these excesses within Beyond the Standard Model (BSM) frameworks featuring a non-SM Higgs state lighter than 125 GeV, i.e., than the one observed at the LHC in 2012 [36, 37].

A possible route to follow in explaining such events through a companion Higgs state (to the 125 GeV one) is to resort to a 2HDM [38, 39], as done, e.g., in Refs. [40–43], wherein a Type-III (which allows direct couplings of both Higgs doublets to all SM fermions) with specific fermion textures was invoked successfully as a BSM explanation to the $b\bar{b}$, $\gamma\gamma$ and $\tau^+\tau^-$ excesses seen at LEP and the LHC. Herein, both a fully CP-even and a mixed CP-even/odd solution was found, upon refining the 2HDM Type-III Yukawa structure to comply with both theoretical consistency requirements and experimental measurements of the discovered Higgs mass and couplings (of the 125 GeV Higgs state).

In this study, we show that solutions of the same kind (i.e., both a fully CP-even and a mixed CP-even/odd one) can also be found in a 2HDM Type-I, wherein only one Higgs doublet gives mass to all SM fermions, again, satisfying the aforementioned theoretical requirements and experimental constraints.

The paper is organised as follows. In the next section, we review the theoretical framework of the 2HDM Type-I. Then we discuss the theoretical and experimental constraints applied to such a BSM scenario in our study, after which we move on to show how the latter can naturally explain the discussed anomalous data in various configurations of its parameters space. Our conclusions then follow.

* khanna_akshat@iitgn.ac.in

† s.moretti@soton.ac.uk; stefano.moretti@physics.uu.se

‡ agnivosarkar@hri.res.in

II. THE 2HDM TYPE-I

Among the various BSM scenarios, the 2HDM can be considered as a simple extension of the SM. The scalar sector of this model comprises two complex scalar fields ϕ_1 and ϕ_2 which transform as a doublet under the Electro-Weak (EW) gauge group $SU(2)_L \times U(1)_Y$ with hypercharge $Y = 1$. For a detailed overview of this model interested reader can look into [44]. The most general gauge invariant CP-conserving scalar potential can be written as

$$\begin{aligned}
 V(\phi_1, \phi_2) = & m_{11}^2 \phi_1^\dagger \phi_1 + m_{22}^2 \phi_2^\dagger \phi_2 - m_{12}^2 \left[\phi_1^\dagger \phi_2 + \phi_2^\dagger \phi_1 \right] + \frac{\lambda_1}{2} (\phi_1^\dagger \phi_1)^2 + \frac{\lambda_2}{2} (\phi_2^\dagger \phi_2)^2 \\
 & + \lambda_3 (\phi_1^\dagger \phi_1) (\phi_2^\dagger \phi_2) + \lambda_4 (\phi_1^\dagger \phi_2) (\phi_2^\dagger \phi_1) + \left[\frac{\lambda_5}{2} (\phi_1^\dagger \phi_2)^2 + h.c. \right] + \left[\lambda_6 (\phi_1^\dagger \phi_1) + \lambda_7 (\phi_2^\dagger \phi_2) \right] (\phi_1^\dagger \phi_2) + h.c. \}.
 \end{aligned} \tag{1}$$

Given the hermiticity of the scalar potential, all the potential parameters of Eq.(1) must be real. In order to prevent tree level Flavour Changing Neutral Currents (FCNCs), one can postulate an additional discrete \mathcal{Z}_2 symmetry under which the scalar fields transform as $\phi_1 \rightarrow \phi_1$, $\phi_2 \rightarrow -\phi_2$. One can realise that the term proportional to m_{12}^2 , λ_6 and λ_7 in Eq.(1) violates this \mathcal{Z}_2 symmetry explicitly. Therefore the potential can be expressed in the following form:

$$\begin{aligned}
 V(\phi_1, \phi_2) = & m_{11}^2 \phi_1^\dagger \phi_1 + m_{22}^2 \phi_2^\dagger \phi_2 + \frac{\lambda_1}{2} (\phi_1^\dagger \phi_1)^2 + \frac{\lambda_2}{2} (\phi_2^\dagger \phi_2)^2 \\
 & + \lambda_3 (\phi_1^\dagger \phi_1) (\phi_2^\dagger \phi_2) + \lambda_4 (\phi_1^\dagger \phi_2) (\phi_2^\dagger \phi_1) + \left\{ \frac{\lambda_5}{2} (\phi_1^\dagger \phi_2)^2 + h.c. \right\}.
 \end{aligned} \tag{2}$$

Both these Higgs fields, ϕ_1 and ϕ_2 acquire a non-zero vacuum expectation value (vev) (i.e., $\langle \phi_1 \rangle = v_1$ and $\langle \phi_2 \rangle = v_2$) and spontaneously break the EW gauge symmetry down to $U(1)_{\text{EM}}$. After the symmetry breaking, the W and Z boson becomes massive and the scalar sector contains five physical Higgs bosons - two CP-even $\{H, h\}$, one CP-odd A and a pair of charged states H^\pm with masses m_H, m_h, m_A and m_{H^\pm} , respectively. Both these vevs v_1 and v_2 are related to the EW scale $v = \sqrt{v_1^2 + v_2^2} = 246$ GeV. The ratio between these two vevs can be parameterised as $\tan \beta = \frac{v_2}{v_1}$. In addition, the mixing angle between the CP-even states $\{H, h\}$ can be parametrised as α . For present study we consider the inverted hierarchy between the CP-even mass eigenstates. This particular choice alters the usual interpretation of the mass spectrum and the couplings¹. Hereafter we align H as to be the SM like Higgs boson and h to be the lighter scalar. In Eq. (3) we present the relations between the potential parameters λ_i 's with the physical parameters of the model:

$$\begin{aligned}
 \lambda_1 &= \frac{c_\alpha^2 m_H^2 + s_\alpha^2 m_h^2}{v^2 c_\beta^2}, \\
 \lambda_2 &= \frac{c_\alpha^2 m_h^2 + s_\alpha^2 m_H^2}{v^2 s_\beta^2}, \\
 \lambda_3 &= \frac{(m_H^2 - m_h^2) s_\alpha c_\alpha - (\lambda_4 + \lambda_5) v^2 c_\beta s_\beta}{v^2 c_\beta s_\beta}, \\
 \lambda_4 &= \frac{m_A^2 - 2m_{H^\pm}^2}{v^2}, \\
 \lambda_5 &= -\frac{m_A^2}{v^2}.
 \end{aligned} \tag{3}$$

The scalar potential given in Eq.(2) clearly has six independent parameters, and the m_{ii}^2 terms can be traded off in terms of λ_i using the extremization conditions on the potential. We find relations of the parameters of the potentials given in equation Eq.(3) in terms of physical scalar masses and the angles $\{\beta, \alpha\}$ and use those as the input parameters for further analysis.

The right handed up/down quarks and lepton fields are also charged under the aforementioned Z_2 symmetry and transform as $u_R^i \rightarrow -u_R^i$, $d_R^i \rightarrow -d_R^i$ and $\ell_R^i \rightarrow -\ell_R^i$, respectively. From these charge assignment one realises that all charged fermions exclusively couple to the Φ_2 field, leading to the traditional 2HDM Type-I scenario. In Eq.(4) we write down the Yukawa part of the Lagrangian in the mass eigenstate basis.

¹ For example, in the inverted mass hierarchy the alignment limit corresponds to $\cos(\beta - \alpha) \rightarrow 1$. However, we will not conform to this limit in the present study.

$$\begin{aligned}
-\mathcal{L}_{Yukawa} = & + \sum_{f=u,d,\ell} \left[m_f f \bar{f} + \left(\frac{m_f}{v} \kappa_h^f \bar{f} f h + \frac{m_f}{v} \kappa_H^f \bar{f} f H - i \frac{m_f}{v} \kappa_A^f \bar{f} \gamma_5 f A \right) \right] \\
& + \frac{\sqrt{2}}{v} \bar{u} (m_u V \kappa_{H^+}^u P_L + V m_d \kappa_{H^+}^d P_R) d H^+ + \frac{\sqrt{2} m_\ell \kappa_{H^+}^\ell}{v} \bar{\nu}_L \ell_R H^+ + h.c.
\end{aligned} \tag{4}$$

Here m_f is the fermion mass, V is the CKM matrix and $P_{L/R} = \frac{1 \pm \gamma_5}{2}$ are the projection operators. The explicit form of the scaling function κ_i are detailed in Table I.

κ_S^i	Coefficient
κ_H^V	$\cos(\beta - \alpha)$
κ_h^V	$\sin(\beta - \alpha)$
κ_H^f	$\frac{\sin \alpha}{\sin \beta}$
κ_h^f	$\frac{\cos \alpha}{\sin \beta}$
κ_A^f	$\cot \beta$
$\kappa_{H^+}^u$	$\cot \beta$
$\kappa_{H^+}^{d/\ell}$	$-\cot \beta$

TABLE I: Explicit form of different coupling modifiers κ_S^i . Here S denotes different scalars in the 2HDM and i can be SM gauge bosons and fermions.

III. CONSTRAINTS

In this section, we describe different theoretical and experimental constraints which are required to restrict the parameter space of the Type-I 2HDM.

A. Theoretical Constraints

- **Vacuum Stability:** The vacuum stability conditions ensure that the potential must be bounded from below in all possible field direction. To achieve these, the λ_i 's parameters must follow certain relationship such that the quartic terms in the potential must dominate in large field values. Here we list down the conditions on λ_i 's which is needed to meet the stability criteria, that prevents the potential from becoming infinitely negative, [45]

$$\lambda_1 > 0, \quad \lambda_2 > 0, \quad \lambda_3 + \sqrt{\lambda_1 \lambda_2} > 0, \quad \lambda_3 + \lambda_4 - |\lambda_5| + \sqrt{\lambda_1 \lambda_2} > 0.$$

- **Unitarity:** The unitarity constraints are necessary to ensure that the theory remains predictive at high energies. At tree level, unitarity imposes specific conditions on the energy growth of all possible $2 \rightarrow 2$ scattering processes. Ref[46, 47] derives the unitarity conditions for the 2HDM model explicitly. According to the unitarity constraint, the following relations should be obeyed:

$$|u_i| \leq 8\pi,$$

where

$$\begin{aligned}
u_1 &= \frac{1}{2}(\lambda_1 + \lambda_2 \pm \sqrt{(\lambda_1 - \lambda_2)^2 + 4|\lambda_5|^2}), \\
u_2 &= \frac{1}{2}(\lambda_1 + \lambda_2 \pm \sqrt{(\lambda_1 - \lambda_2)^2 + 4\lambda_4^2}), \\
u_3 &= \frac{1}{2}(3(\lambda_1 + \lambda_2) \pm \sqrt{9(\lambda_1 - \lambda_2)^2 + 4(2\lambda_3 + \lambda_4)^2}), \\
u_4 &= \lambda_3 + 2\lambda_4 \pm 3|\lambda_5|, \\
u_5 &= \lambda_3 \pm |\lambda_5|, \\
u_6 &= \lambda_3 \pm \lambda_4.
\end{aligned}$$

- **Perturbativity:** The perturbativity condition on the parameters of the scalar potential, which imposes an upper limit on all the quartic couplings, demands that, for all i values, one has $\lambda_i \leq |4\pi|$.

B. Experimental Constraints

- **EW Precision Tests** We evaluated the EW precision constraints by computing the S, T and U parameters using the SPheno package [48], with the model files written in SARAH [49]. These so-called ‘oblique parameters’ provide stringent constraints on new physics, thereby demanding that any extension to the SM Higgs sector should conform to high precision data from LEP (primarily). The numerical values of these observables are [50]

$$S = -0.02 \pm 0.10, \quad T = 0.03 \pm 0.12, \quad U = 0.01 \pm 0.11.$$

- **BSM Higgs Boson Exclusion** We assessed the exclusion limits from direct searches for the BSM scalars at the LHC, LEP and the Tevatron. These exclusion limits were evaluated at the 95% Confidence Level (C.L.) using the HiggsBounds-6 [51] module via the HiggsTools [52] package. In our analysis we have also demanded that our lighter Higgs must comply with the results of [53], where the scalars are produced in association with a massive vector boson or a top anti-quark pair and further decays via leptonic modes.
- **SM-Like Higgs Boson Discovery** We examined the compatibility of our 125 GeV Higgs boson with the discovered SM-like Higgs boson using a goodness-of-fit test. Specifically, we calculated the χ -square value with HiggsSignals-3 [54] via HiggsTools, comparing the predicted signal strengths of our Higgs boson to those observed experimentally. We retained the parameter spaces that satisfies the condition $\chi_{125}^2 < 189.42$, corresponding to a 95% C.L. with 159 degrees of freedom.
- **Flavour Physics** We incorporated constraints from B -physics observables, which are sensitive to potential new physics contributions in loop mediated FCNC processes. Specifically, we tested the most stringent bound on the Branching Ratio (\mathcal{BR}) of the $B \rightarrow X_s \gamma$ decay using Next-to-Leading Order (NLO) calculations in QCD as discussed in [55].

$$\mathcal{BR}(B \rightarrow X_s \gamma) = \frac{\Gamma(B \rightarrow X_s \gamma)}{\Gamma_{SL}} \mathcal{BR}_{SL} \quad (5)$$

where, \mathcal{BR}_{SL} is the semi-leptonic branching ratio and Γ_{SL} is the semi-leptonic decay width.

We took our input parameters from the most recent values from the Particle Data Group (PDG) compilation [50], as follows:

$$\begin{aligned} \alpha_s(M_Z) &= 0.1179 \pm 0.0010, & m_t &= 172.76 \pm 0.3, \\ \frac{m_b}{m_c} &= 4.58 \pm 0.01, & \alpha &= \frac{1}{137.036}, \\ \mathcal{BR}_{SL} &= 0.1049 \pm 0.0046, & \left| \frac{V_{ts}^* V_{tb}}{V_{cb}} \right|^2 &= 0.95 \pm 0.02, \\ m_b(\overline{MS}) &= 4.18 \pm 0.03, & m_c &= 1.27 \pm 0.02, \\ m_Z &= 91.1876 \pm 0.0021, & m_W &= 86.377 \pm 0.012. \end{aligned}$$

The following restriction has been imposed, which represents the 3σ experimental limit:

$$2.87 \times 10^{-4} < \mathcal{BR}(B \rightarrow X_s \gamma) < 3.77 \times 10^{-4}.$$

Other B -physics observables, like $\mathcal{BR}(B^+ \rightarrow \tau^+ \nu_\tau)$, $\mathcal{BR}(D_s \rightarrow \tau \nu_\tau)$, $\mathcal{BR}(B_s \rightarrow \mu^+ \mu^-)$ and $\mathcal{BR}(B^0 \rightarrow \mu^+ \mu^-)$ have been taken care of by using the FlavorKit tool [56] provided by SPheno package [48]. Our calculated $b \rightarrow s \gamma$ results were also found to be consistent with the FlavorKit tool.

IV. EXPLAINING THE ANOMALIES

The primary objective of this paper is to investigate whether the 2HDM Type-I can explain the excesses observed at the LHC and LEP data over the 92 – 98 GeV or so mass range. To do so, we need to define the signal strength corresponding to these three excesses. The signal strength is formulated as a ratio between the observed number of events to the expected number of events for a hypothetical SM Higgs of mass 95 GeV. Assuming the Narrow Width Approximation (NWA), the signal strength for the $\tau^+\tau^-$, $\gamma\gamma$ and $b\bar{b}$ channels can be parameterised as cross section (σ) times the branching ratio (\mathcal{BR}),

$$\begin{aligned}\mu_{\tau^+\tau^-}(\phi) &= \frac{\sigma_{2\text{HDM}}(gg \rightarrow \phi)}{\sigma_{\text{SM}}(gg \rightarrow h_{\text{SM}})} \times \frac{\mathcal{BR}_{2\text{HDM}}(\phi \rightarrow \tau^+\tau^-)}{\mathcal{BR}_{\text{SM}}(h_{\text{SM}} \rightarrow \tau^+\tau^-)}, \\ \mu_{\gamma\gamma}(\phi) &= \frac{\sigma_{2\text{HDM}}(gg \rightarrow \phi)}{\sigma_{\text{SM}}(gg \rightarrow h_{\text{SM}})} \times \frac{\mathcal{BR}_{2\text{HDM}}(\phi \rightarrow \gamma\gamma)}{\mathcal{BR}_{\text{SM}}(h_{\text{SM}} \rightarrow \gamma\gamma)}, \\ \mu_{b\bar{b}}(\phi) &= \frac{\sigma_{2\text{HDM}}(e^+e^- \rightarrow Z\phi)}{\sigma_{\text{SM}}(e^+e^- \rightarrow Zh_{\text{SM}})} \times \frac{\mathcal{BR}_{2\text{HDM}}(\phi \rightarrow b\bar{b})}{\mathcal{BR}_{\text{SM}}(h_{\text{SM}} \rightarrow b\bar{b})}.\end{aligned}\tag{6}$$

Here, h_{SM} corresponds to a SM like Higgs Boson with a mass of 95 GeV while ϕ is a 2HDM Type-I Higgs state with the same mass. The experimental measurements for these three signal strengths around 95 GeV are expressed as

$$\begin{aligned}\mu_{\gamma\gamma}^{\text{exp}} &= \mu_{\gamma\gamma}^{\text{ATLAS+CMS}} = 0.24_{-0.08}^{+0.09}, \quad [3, 57, 58] \\ \mu_{\tau^+\tau^-}^{\text{exp}} &= 1.2 \pm 0.5, \quad [59] \\ \mu_{b\bar{b}}^{\text{exp}} &= 0.117 \pm 0.057. \quad [1, 60]\end{aligned}\tag{7}$$

Although the ditau excess is most prominent around 100 GeV and the $b\bar{b}$ excess near 98 GeV, a search around 95 GeV could provide a unified explanation for all these three anomalies. This is because the mass resolution in the ditau final states is substantially large, and the LEP excess, associated with the $b\bar{b}$ final states, is also broad. Therefore, a common origin for these excesses may plausibly reside around 95 GeV.

In our analysis, we have combined the di-photon measurements from the ATLAS and CMS experiments, denoted as $\mu_{\gamma\gamma}^{\text{ATLAS}}$ and $\mu_{\gamma\gamma}^{\text{CMS}}$, respectively. The ATLAS measurement yields a central value of 0.18 ± 0.1 [61] while the CMS measurement yields a central value of $0.33_{-0.12}^{+0.19}$ [62]. The combined measurement, denoted by $\mu_{\gamma\gamma}^{\text{ATLAS+CMS}}$ is determined by taking the average of these two central values, assuming both these measurements are uncorrelated. The corresponding combined uncertainty is calculated by adding corresponding uncertainties in quadrature. To determine if the observed excess can be explained through our model or otherwise, we perform a χ^2 analysis using the central values μ^{exp} and the 1σ uncertainties $\Delta\mu^{\text{exp}}$ associated with the signal related to the excesses as defined in Eq. (7). The contribution to the χ^2 for each of the channel is calculated using the equation

$$\chi_{\gamma\gamma, \tau^+\tau^-, b\bar{b}}^2 = \frac{(\mu_{\gamma\gamma, \tau^+\tau^-, b\bar{b}}(\phi) - \mu_{\gamma\gamma, \tau^+\tau^-, b\bar{b}}^{\text{exp}})^2}{(\Delta\mu_{\gamma\gamma, \tau^+\tau^-, b\bar{b}}^{\text{exp}})^2}.\tag{8}$$

Hence, the resulting χ^2 which we will use to determine if the excesses are explained by the 2HDM Type-I, or otherwise, is the following:

$$\chi_{\gamma\gamma, \tau^+\tau^-, b\bar{b}}^2 = \chi_{\gamma\gamma}^2 + \chi_{\tau^+\tau^-}^2 + \chi_{b\bar{b}}^2.\tag{9}$$

We test this BSM scenario into two cases: firstly, we consider both the CP-even and CP-odd (i.e., $\phi = h + A$. except for $b\bar{b}$ where $\phi = h$) Higgs states simultaneously in explaining the anomaly and, secondly, we only exploit the CP-even Higgs (i.e., $\phi = h$) in order to explain it. Hence, we align our H state (recall that we have $m_h < m_H$) with the SM Higgs boson, so that $m_H = 125$ GeV, and start a Monte Carlo (MC) sampling of the various input parameters.

A. The Overlapping Solution

In case of overlapping solution, the signal strength corresponding to the $\tau^+\tau^-$ and $\gamma\gamma$ channels receive substantial contribution from both the CP-even and CP-odd states simultaneously². In contrast, for the $b\bar{b}$ mode only the CP-even

² Here we have considered CP-conserving potential. As a result, the h and A states would not interfere with each other.

Parameter	Scan Range
m_H	125
m_h	92 – 98
m_A	92 – 98
m_{H^\pm}	80 – 230
$\tan\beta$	0.5 – 100
$\sin(\beta - \alpha)$	-0.66 – 0.62

TABLE II: The scan range which is used for the MC sampling. All the Masses are in GeV.

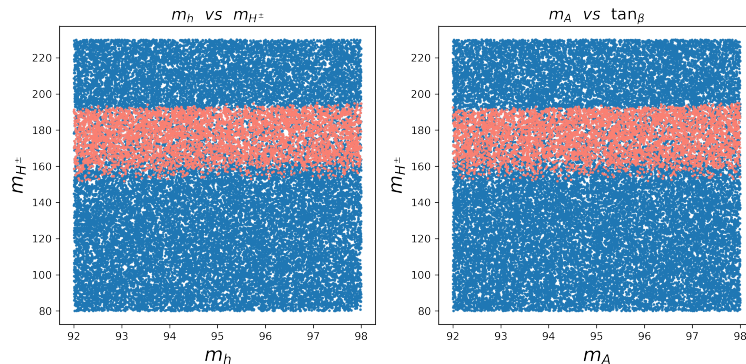


FIG. 1: Results of the scan in Table II mapped against the Higgs masses. The blue regions are allowed by stability, unitarity and perturbativity constraints while the red regions are allowed by Higgs data, $b \rightarrow s\gamma$ and EW precision constraints.

state contribute as the trilinear coupling AZZ is zero at tree level. As a result, the signal strength can be expressed in the following manner -

$$\mu_{\tau+\tau^-}(h+A) = \mu_{\tau+\tau^-}(h) + \mu_{\tau+\tau^-}(A), \quad \mu_{\gamma\gamma}(h+A) = \mu_{\gamma\gamma}(h) + \mu_{\gamma\gamma}(A), \quad \mu_{b\bar{b}}(h).$$

We generated MC samples in the scan range as described in Table II. After testing them against various theoretical and experimental constraints, the allowed parameter space is illustrated in Figure 1. The region of the parameter space that pass the theoretical constraints are depicted by the blue points while the region that pass the experimental constraints are depicted by the red points. The plot illustrates that a nearly degenerate solution with both the CP-even and CP-odd Higgs in the 92–98 GeV mass range is viable for the charged Higgs mass ranging around $160 < m_{H^\pm} < 195$. We will use the overlapping region of the two coloured point distributions to test the aforementioned anomalies.

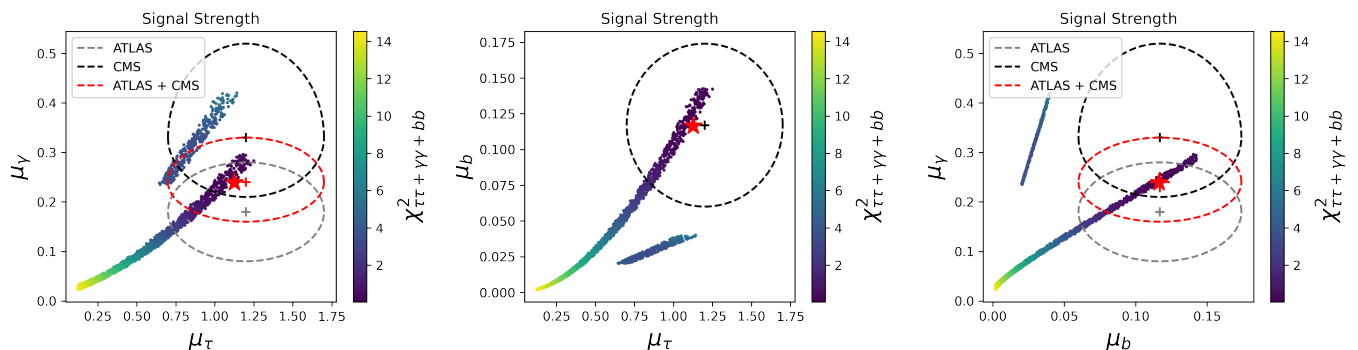


FIG. 2: Correlations amongst the signal strengths in Eq. (6). Here, the total χ^2 is displayed using the colour bar and the best fit point is given by star marker. The ATLAS and CMS results with their corresponding 1σ band is also represented.

Figure 2 illustrates the total chi-square distribution for points that are compatible with all three anomalies and

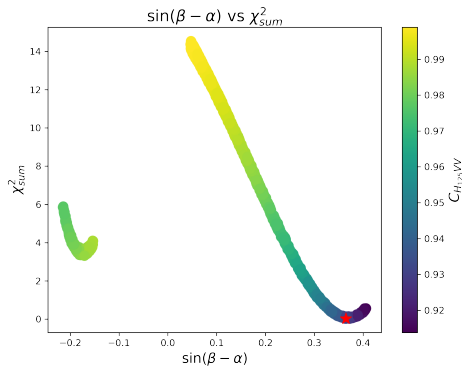


FIG. 3: $\sin(\beta - \alpha)$ plotted against χ_{sum}^2 . The χ_{min}^2 is indicated by a star.

the best fit point is marked by a star, corresponding to χ_{min}^2 . The experimentally observed signal strength with their 1σ band is also superimposed in the plot to test them against this model's best fit point. The chi-square fit reveals two distinct branches, differentiated by the sign of $\sin(\beta - \alpha)$. The main branch, characterized by positive values, is densely populated, while the second branch, which has negative values, is sparsely populated due to the elimination of many points by various constraints. The figure 3 also illustrates the sign of the electroweak coupling parameter. The best fit point indicated by a red star has a large positive $\sin(\beta - \alpha)$ value, while the vector boson coupling with the SM Higgs boson, indicated by the color bar, is weakened in that case.

Given that the di-photon excess is most pronounced around 95 GeV, we also plot the allowed points within the 94 – 96 GeV range over the CMS and ATLAS results for the signal strength in the $\gamma\gamma$ channel, as shown in Figure 4. The expected and observed CMS limits are shown by the black dashed and solid lines. The green and yellow bands indicate the 1σ and 2σ uncertainties and the plot is overlaid by the ATLAS observed 95% confidence level limits on the signal strength with the red dashed and solid lines. The combined signal strength (CMS+ATLAS) at 95.4 GeV with its error bar is also shown using a red dot. The points explaining the anomaly at the 1σ level, for 3 degrees of freedom, corresponding to the $\gamma\gamma$, $\tau\tau$ and $b\bar{b}$ channels as shown in equation 9, which requires $\chi^2 < 3.53$, are plotted in dark red while the points explaining it at the 3σ level, demanding $\chi^2 < 7.8147$ are shown in peru color (Less likely points are given in sky blue). The best fit point in the 94 – 96 range is also indicated using midnight blue color. It can be clearly seen that the parameter points are suited to explain the excesses observed. The details of the best fit points as marked in the two figures are shown in Table III.

B. The Single Solution

In this case, only the h state is responsible for explaining all the three anomalies. We sampled points for the scan range described in Table IV, and the points that pass the various constraints are depicted in Figure 5, wherein the blue shaded region indicates the points that pass the various theoretical constraints while the red shaded region indicates region of parameter space that survives after imposing different experimental bounds. The plots clearly represent the allowed parameter space for the CP-odd and Charged Higgs masses, given that we fix our CP-even mass to lie in the range 92 – 97 GeV. Though the charged Higgs mass is bounded at around 160 GeV, the CP-odd pseudoscalar covers almost the entire scan range. Note that the allowed CP-odd scalar mass also lie in the 90 – 100 GeV mass window, hinting to the overlapping solution that we discussed in the previous section. We move ahead with testing the overlapping points with the observed anomalies.

The total χ^2 fit for the points passing all the constraints is displayed in Figure 6, wherein the best fit point (i.e., again, the χ_{min}^2 one) is indicated with a star. We have again overlaid the plot with the experimentally observed data

Parameter	m_H	m_h	m_A	m_{H^\pm}	$\tan\beta$	$\sin(\beta - \alpha)$	$\mu_{\tau^+\tau^-}(h + A)$	$\mu_{\gamma\gamma}(h + A)$	$\mu_{b\bar{b}}(h)$	$\chi_{\tau^+\tau^-+\gamma\gamma+b\bar{b}}^2$
Fig 2	125.0	92.23	92.21	176.81	3.26	0.36	1.1255	0.2395	0.1164	0.02235
Fig 4	125.0	94.03	95.71	191.77	3.22	0.38	1.107	0.2510	0.1228	0.0598

TABLE III: BPs extracted from Figures 2 and 4. Masses are in GeV.

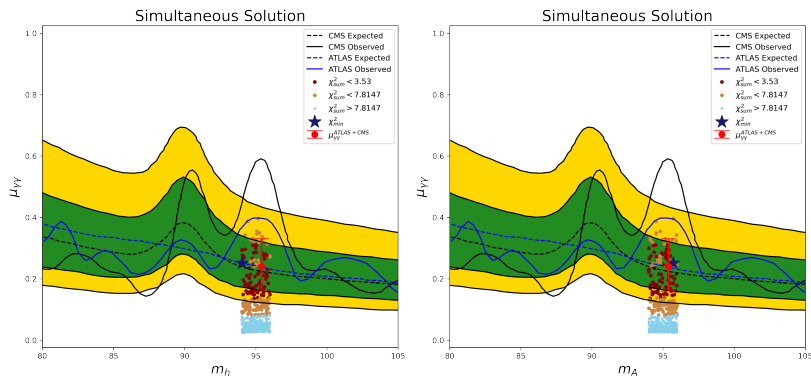


FIG. 4: The di-photon signal strength results from experiment tensioned against the 2HDM Type-I predictions satisfying the three anomalies simultaneously.

Parameter	Scan Range
m_H	125
m_h	92 – 97
m_A	80 – 230
m_{H^\pm}	80 – 230
$\tan\beta$	0.5 – 100
$\sin(\beta - \alpha)$	-0.66 – 0.62

TABLE IV: The scan range which is used for the MC sampling. All the Masses are in GeV.

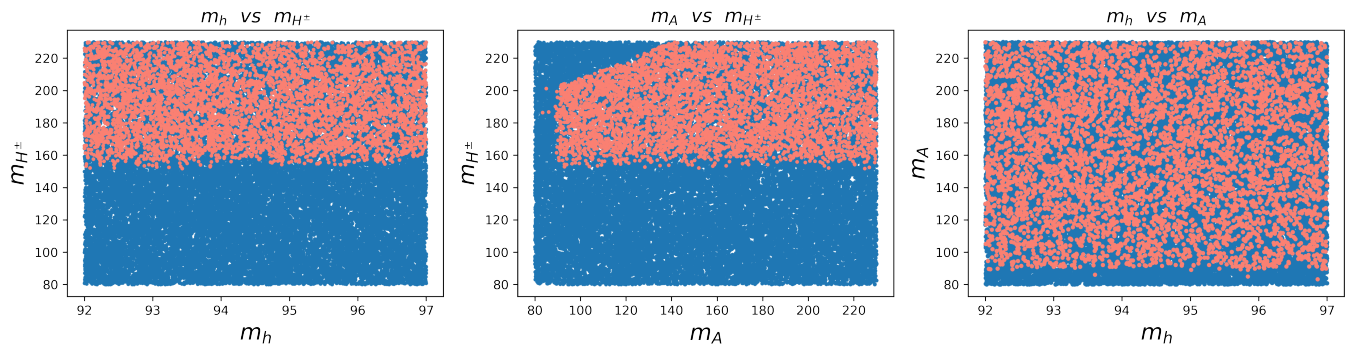


FIG. 5: Results of the scan in Table IV mapped against the Higgs masses. The blue regions are allowed by stability, unitarity and perturbativity constraints while the red regions are allowed by Higgs data, $b \rightarrow s\gamma$ and EW precision constraints.

with the 1σ band. The plot clearly depicts that the best fit point lies within the experimental 1σ boundary. The two bands here again are differentiated with the sign of $\sin(\beta - \alpha)$, wherein the densely populated region is positive while the sparsely populated one negative. This is also depicted in Figure 7, where the best fit point is depicted by a red star, which has a large $\sin(\beta - \alpha)$ value, while the vector boson coupling with the SM Higgs boson is weakened, which is indicated by the color bar. The mass region lying between 94 – 96 GeV is also displayed on top of the CMS and ATLAS results for the signal strength in the $\gamma\gamma$ channel in Figure 8 (with the same color coding as that in Figure 4). The figure clearly depicts the best fit point in that particular region to be close to the mean experimentally observed value. Finally the best fit BPs in these cases are shown in Table V.

	m_H	m_h	m_A	m_{H^\pm}	$\tan\beta$	$\sin(\beta - \alpha)$	$\mu_{\tau^+\tau^-}(h)$	$\mu_{\gamma\gamma}(h)$	$\mu_{b\bar{b}}(h)$	$\chi^2_{\tau^+\tau^-+\gamma\gamma+b\bar{b}}$
Figure 6	125.0	92.52	124.73	181.77	3.11	0.41	0.8429	0.1942	0.1457	1.022
Figure 8	125.0	95.84	85.03	201.35	3.11	0.41	0.6631	0.2240	0.2351	1.122

TABLE V: The details of the best fit points extracted from Figures 6 and 8. Masses are in GeV.

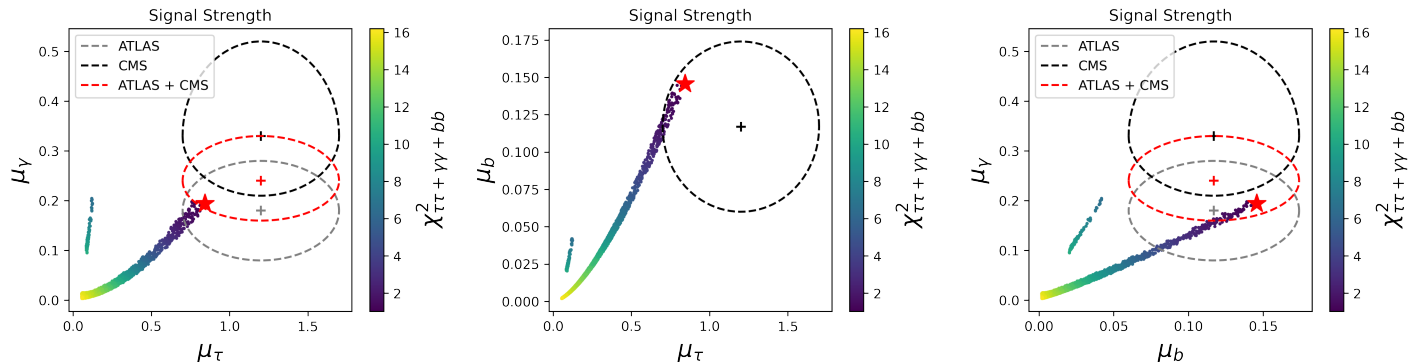


FIG. 6: Correlations amongst the signal strengths in Eq. (6). Here, the total χ^2 is displayed using the colour bar and the best fit point is given by star marker. ATLAS and CMS results with their corresponding 1σ band is also added.

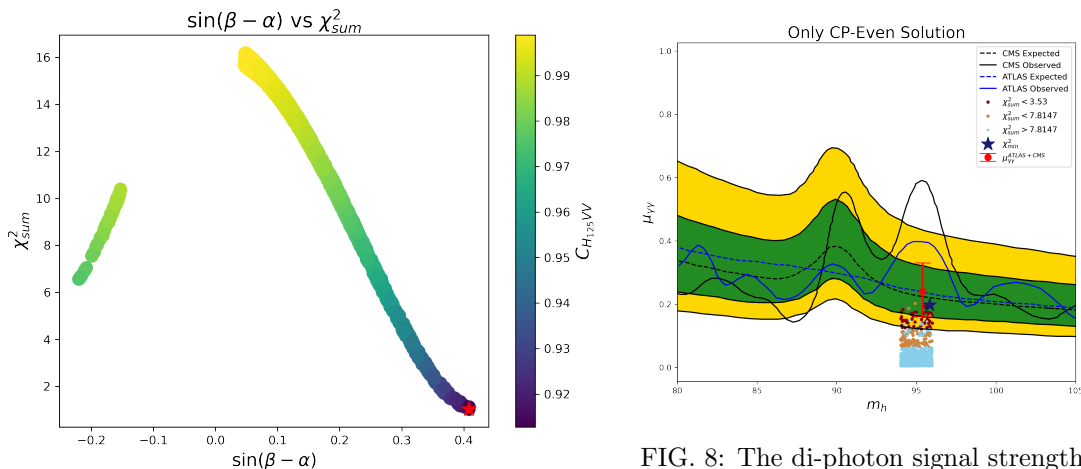


FIG. 7: $\sin(\beta - \alpha)$ plotted against χ^2_{sum} . The best fit point is indicated by a red star.

FIG. 8: The di-photon signal strength results from experiment tensioned against the 2HDM Type-I predictions satisfying the three anomalies simultaneously.

V. CONCLUSIONS

In summary, we have proven that somewhat anomalous data produced at LEP and the LHC in $b\bar{b}$ and $\tau^+\tau^-$ as well as $\gamma\gamma$ final states, respectively, all clustering in a 10 GeV or so mass window around 95 GeV, are consistent with the possibility of the 2HDM-Type I in inverted mass hierarchy explaining these. Specifically, two configurations are possible: one where both the (degenerate) h and A states cooperate to explain the aforementioned anomalies and another where only the h states does so. This is an intriguing result, as such Higgs states can well be probed in collateral signatures specific to the 2HDM Type-I in inverted mass hierarchy, as emphasised in various previous literature [63–70]. To aid testing this theoretical hypothesis, we have produced two pairs of BPs amenable to further phenomenological analysis, each pair corresponding to one of the above two solutions, wherein the parameter space point giving the best fit to all anomalies.

ACKNOWLEDGMENTS

The work of S.M. is supported in part through the NExT Institute and the STFC Consolidated Grant No. ST/L000296/1. A.S acknowledges the support from SERB-National Postdoctoral fellowship (Ref No: PDF/2023/002572). A.K. acknowledges the support from Director's Fellowship at IIT Gandhinagar. All authors thank Tanmoy Mondal and Prasenjit Sanyal for their help in discovering a mistake in their calculations.

-
- [1] R. Barate *et al.* (LEP Working Group for Higgs boson searches, ALEPH, DELPHI, L3, OPAL), Search for the standard model Higgs boson at LEP, *Phys. Lett. B* **565**, 61 (2003), [arXiv:hep-ex/0306033](#).
- [2] S. Schael *et al.* (ALEPH, DELPHI, L3, OPAL, LEP Working Group for Higgs Boson Searches), Search for neutral MSSM Higgs bosons at LEP, *Eur. Phys. J. C* **47**, 547 (2006), [arXiv:hep-ex/0602042](#).
- [3] A. M. Sirunyan *et al.* (CMS), Search for a standard model-like Higgs boson in the mass range between 70 and 110 GeV in the diphoton final state in proton-proton collisions at $\sqrt{s} = 8$ and 13 TeV, *Phys. Lett. B* **793**, 320 (2019), [arXiv:1811.08459 \[hep-ex\]](#).
- [4] Search for a standard model-like Higgs boson in the mass range between 70 and 110 GeV in the diphoton final state in proton-proton collisions at $\sqrt{s} = 13$ TeV, <https://cds.cern.ch/record/2852907/>, CERN, Geneva (2023).
- [5] J. Cao, X. Guo, Y. He, P. Wu, and Y. Zhang, Diphoton signal of the light Higgs boson in natural NMSSM, *Phys. Rev. D* **95**, 116001 (2017), [arXiv:1612.08522 \[hep-ph\]](#).
- [6] S. Heinemeyer, C. Li, F. Lika, G. Moortgat-Pick, and S. Paasch, Phenomenology of a 96 GeV Higgs boson in the 2HDM with an additional singlet, *Phys. Rev. D* **106**, 075003 (2022), [arXiv:2112.11958 \[hep-ph\]](#).
- [7] T. Biekötter, A. Grohsjean, S. Heinemeyer, C. Schwanenberger, and G. Weiglein, Possible indications for new Higgs bosons in the reach of the LHC: N2HDM and NMSSM interpretations, *Eur. Phys. J. C* **82**, 178 (2022), [arXiv:2109.01128 \[hep-ph\]](#).
- [8] T. Biekötter, M. Chakraborti, and S. Heinemeyer, A 96 GeV Higgs boson in the N2HDM, *Eur. Phys. J. C* **80**, 2 (2020), [arXiv:1903.11661 \[hep-ph\]](#).
- [9] J. Cao, X. Jia, Y. Yue, H. Zhou, and P. Zhu, 96 GeV diphoton excess in seesaw extensions of the natural NMSSM, *Phys. Rev. D* **101**, 055008 (2020), [arXiv:1908.07206 \[hep-ph\]](#).
- [10] T. Biekötter, S. Heinemeyer, and G. Weiglein, Excesses in the low-mass Higgs-boson search and the W -boson mass measurement, *Eur. Phys. J. C* **83**, 450 (2023), [arXiv:2204.05975 \[hep-ph\]](#).
- [11] S. Iguro, T. Kitahara, and Y. Omura, Scrutinizing the 95 – 100 GeV di-tau excess in the top associated process, *Eur. Phys. J. C* **82**, 1053 (2022), [arXiv:2205.03187 \[hep-ph\]](#).
- [12] W. Li, J. Zhu, K. Wang, S. Ma, P. Tian, and H. Qiao, A light Higgs boson in the NMSSM confronted with the CMS di-photon and di-tau excesses, (2022), [arXiv:2212.11739 \[hep-ph\]](#).
- [13] J. M. Cline and T. Toma, Pseudo-Goldstone dark matter confronts cosmic ray and collider anomalies, *Phys. Rev. D* **100**, 035023 (2019), [arXiv:1906.02175 \[hep-ph\]](#).
- [14] T. Biekötter and M. O. Olea-Romacho, Reconciling Higgs physics and pseudo-Nambu-Goldstone dark matter in the S2HDM using a genetic algorithm, *JHEP* **10**, 215, [arXiv:2108.10864 \[hep-ph\]](#).
- [15] A. Crivellin, J. Heeck, and D. Müller, Large $h \rightarrow bs$ in generic two-Higgs-doublet models, *Phys. Rev. D* **97**, 035008 (2018), [arXiv:1710.04663 \[hep-ph\]](#).
- [16] G. Cacciapaglia, A. Deandrea, S. Gascon-Shotkin, S. Le Corre, M. Lethuillier, and J. Tao, Search for a lighter Higgs boson in Two Higgs Doublet Models, *JHEP* **12**, 068, [arXiv:1607.08653 \[hep-ph\]](#).
- [17] A. A. Abdelalim, B. Das, S. Khalil, and S. Moretti, Di-photon decay of a light Higgs state in the BLSSM, *Nucl. Phys. B* **985**, 116013 (2022), [arXiv:2012.04952 \[hep-ph\]](#).
- [18] T. Biekötter, S. Heinemeyer, and G. Weiglein, Mounting evidence for a 95 GeV Higgs boson, *JHEP* **08**, 201, [arXiv:2203.13180 \[hep-ph\]](#).
- [19] T. Biekötter, S. Heinemeyer, and G. Weiglein, The CMS di-photon excess at 95 GeV in view of the LHC Run 2 results, *Phys. Lett. B* **846**, 138217 (2023), [arXiv:2303.12018 \[hep-ph\]](#).
- [20] D. Azevedo, T. Biekötter, and P. M. Ferreira, 2HDM interpretations of the CMS diphoton excess at 95 GeV, *JHEP* **11**, 017, [arXiv:2305.19716 \[hep-ph\]](#).
- [21] T. Biekötter, S. Heinemeyer, and G. Weiglein, 95.4 GeV diphoton excess at ATLAS and CMS, *Phys. Rev. D* **109**, 035005 (2024), [arXiv:2306.03889 \[hep-ph\]](#).
- [22] J. Cao, X. Jia, and J. Lian, Unified Interpretation of Muon $g-2$ anomaly, 95 GeV Diphoton, and $b\bar{b}$ Excesses in the General Next-to-Minimal Supersymmetric Standard Model, (2024), [arXiv:2402.15847 \[hep-ph\]](#).
- [23] K. Wang and J. Zhu, A 95 GeV light Higgs in the top-pair-associated diphoton channel at the LHC in the Minimal Dilaton Model, (2024), [arXiv:2402.11232 \[hep-ph\]](#).
- [24] W. Li, H. Qiao, K. Wang, and J. Zhu, Light dark matter confronted with the 95 GeV diphoton excess, (2023), [arXiv:2312.17599 \[hep-ph\]](#).
- [25] P. S. B. Dev, R. N. Mohapatra, and Y. Zhang, Explanation of the 95 GeV $\gamma\gamma$ and $b\bar{b}$ excesses in the minimal left-right symmetric model, *Phys. Lett. B* **849**, 138481 (2024), [arXiv:2312.17733 \[hep-ph\]](#).
- [26] D. Borah, S. Mahapatra, P. K. Paul, and N. Sahu, Scotogenic $U(1)_{L\mu-L\tau}$ origin of $(g-2)_\mu$, W -mass anomaly and 95 GeV excess, *Phys. Rev. D* **109**, 055021 (2024), [arXiv:2310.11953 \[hep-ph\]](#).

- [27] J. Cao, X. Jia, J. Lian, and L. Meng, 95 GeV diphoton and $b\bar{b}$ excesses in the general next-to-minimal supersymmetric standard model, *Phys. Rev. D* **109**, 075001 (2024), [arXiv:2310.08436 \[hep-ph\]](#).
- [28] U. Ellwanger and C. Hugonie, Additional Higgs Bosons near 95 and 650 GeV in the NMSSM, *Eur. Phys. J. C* **83**, 1138 (2023), [arXiv:2309.07838 \[hep-ph\]](#).
- [29] J. A. Aguilar-Saavedra, H. B. Camara, F. R. Joaquim, and J. F. Seabra, Confronting the 95 GeV excesses within the $U(1)^\prime$ -extended next-to-minimal 2HDM, *Phys. Rev. D* **108**, 075020 (2023), [arXiv:2307.03768 \[hep-ph\]](#).
- [30] S. Ashanujjaman, S. Banik, G. Coloretti, A. Crivellin, B. Mellado, and A.-T. Mulaudzi, $SU(2)_L$ triplet scalar as the origin of the 95 GeV excess?, *Phys. Rev. D* **108**, L091704 (2023), [arXiv:2306.15722 \[hep-ph\]](#).
- [31] J. Dutta, J. Lahiri, C. Li, G. Moortgat-Pick, S. F. Tabira, and J. A. Ziegler, Dark Matter Phenomenology in 2HDMS in light of the 95 GeV excess, (2023), [arXiv:2308.05653 \[hep-ph\]](#).
- [32] U. Ellwanger and C. Hugonie, NMSSM with correct relic density and an additional 95 GeV Higgs boson, (2024), [arXiv:2403.16884 \[hep-ph\]](#).
- [33] M. A. Diaz, G. Cerro, S. Dasmahapatra, and S. Moretti, Bayesian Active Search on Parameter Space: a 95 GeV Spin-0 Resonance in the $(B - L)$ SSM, (2024), [arXiv:2404.18653 \[hep-ph\]](#).
- [34] U. Ellwanger, C. Hugonie, S. F. King, and S. Moretti, NMSSM Explanation for Excesses in the Search for Neutralinos and Charginos and a 95 GeV Higgs Boson, (2024), [arXiv:2404.19338 \[hep-ph\]](#).
- [35] S. Y. Ayazi, M. Hosseini, S. Paktinat Mehdiabadi, and R. Rouzbehi, The Vector Dark Matter, LHC Constraints Including a 95 GeV Light Higgs Boson, (2024), [arXiv:2405.01132 \[hep-ph\]](#).
- [36] G. Aad *et al.* (ATLAS), Observation of a new particle in the search for the Standard Model Higgs boson with the ATLAS detector at the LHC, *Phys. Lett. B* **716**, 1 (2012), [arXiv:1207.7214 \[hep-ex\]](#).
- [37] S. Chatrchyan *et al.* (CMS), Observation of a New Boson at a Mass of 125 GeV with the CMS Experiment at the LHC, *Phys. Lett. B* **716**, 30 (2012), [arXiv:1207.7235 \[hep-ex\]](#).
- [38] J. F. Gunion, H. E. Haber, G. L. Kane, and S. Dawson, Errata for the Higgs hunter's guide, (1992), [arXiv:hep-ph/9302272](#).
- [39] G. C. Branco, P. M. Ferreira, L. Lavoura, M. N. Rebelo, M. Sher, and J. P. Silva, Theory and phenomenology of two-Higgs-doublet models, *Phys. Rept.* **516**, 1 (2012), [arXiv:1106.0034 \[hep-ph\]](#).
- [40] R. Benbrik, M. Boukidi, S. Moretti, and S. Semlali, Explaining the 96 GeV Di-photon anomaly in a generic 2HDM Type-III, *Phys. Lett. B* **832**, 137245 (2022), [arXiv:2204.07470 \[hep-ph\]](#).
- [41] R. Benbrik, M. Boukidi, S. Moretti, and S. Semlali, Probing a 96 GeV Higgs Boson in the Di-Photon Channel at the LHC, *PoS ICHEP2022*, 547 (2022), [arXiv:2211.11140 \[hep-ph\]](#).
- [42] A. Belyaev, R. Benbrik, M. Boukidi, M. Chakraborti, S. Moretti, and S. Semlali, Explanation of the Hints for a 95 GeV Higgs Boson within a 2-Higgs Doublet Model, (2023), [arXiv:2306.09029 \[hep-ph\]](#).
- [43] R. Benbrik, M. Boukidi, and S. Moretti, Superposition of CP-Even and CP-Odd Higgs Resonances: Explaining the 95 GeV Excesses within a Two-Higgs Doublet Model, (2024), [arXiv:2405.02899 \[hep-ph\]](#).
- [44] G. Branco, P. Ferreira, L. Lavoura, M. Rebelo, M. Sher, and J. P. Silva, Theory and phenomenology of two-higgs-doublet models, *Physics Reports* **516**, 1–102 (2012).
- [45] B. Coleppa, F. Kling, and S. Su, Constraining type ii 2hdm in light of lhc higgs searches, *Journal of High Energy Physics* **2014**, 10.1007/jhep01(2014)161 (2014).
- [46] I. F. Ginzburg and I. P. Ivanov, Tree-level unitarity constraints in the most general two higgs doublet model, *Physical Review D* **72**, 10.1103/physrevd.72.115010 (2005).
- [47] G. Bhattacharyya and D. Das, Scalar sector of two-Higgs-doublet models: A minireview, *Pramana* **87**, 40 (2016), [arXiv:1507.06424 \[hep-ph\]](#).
- [48] W. Porod, SpHeno, a program for calculating supersymmetric spectra, susy particle decays and susy particle production at $e+e-$ colliders, *Computer Physics Communications* **153**, 275–315 (2003).
- [49] F. Staub, Exploring new models in all detail with `ttjsarahj/ttj`, *Advances in High Energy Physics* **2015**, 1–126 (2015).
- [50] R. L. Workman and Others (Particle Data Group), Review of Particle Physics, *PTEP* **2022**, 083C01 (2022).
- [51] P. Bechtel, D. Dercks, S. Heinemeyer, T. Klingl, T. Stefaniak, G. Weiglein, and J. Wittbrodt, Higgsbounds-5: testing higgs sectors in the lhc 13 tev era, *The European Physical Journal C* **80**, 10.1140/epjc/s10052-020-08557-9 (2020).
- [52] H. Bahl, T. Biekotter, S. Heinemeyer, C. Li, S. Paasch, G. Weiglein, and J. Wittbrodt, Higgstools: Bsm scalar phenomenology with new versions of higgsbounds and higgssignals, *Computer Physics Communications* **291**, 108803 (2023).
- [53] A. Tumasyan *et al.* (CMS), Search for a scalar or pseudoscalar dilepton resonance produced in association with a massive vector boson or top quark-antiquark pair in multilepton events at $s=13$ TeV, *Phys. Rev. D* **110**, 012013 (2024), [arXiv:2402.11098 \[hep-ex\]](#).
- [54] P. Bechtel, S. Heinemeyer, T. Klingl, T. Stefaniak, G. Weiglein, and J. Wittbrodt, Higgssignals-2: probing new physics with precision higgs measurements in the lhc 13 tev era, *The European Physical Journal C* **81**, 10.1140/epjc/s10052-021-08942-y (2021).
- [55] F. M. Borzumati and C. Greub, Two higgs doublet model predictions for $b \rightarrow x_s \gamma$ in nlo qcd, *Physical Review D* **58**, 10.1103/physrevd.58.074004 (1998).
- [56] W. Porod, F. Staub, and A. Vicente, A flavor kit for bsm models, *The European Physical Journal C* **74**, 10.1140/epjc/s10052-014-2992-2 (2014).
- [57] *Search for a standard model-like Higgs boson in the mass range between 70 and 110 GeV in the diphoton final state in proton-proton collisions at $\sqrt{s} = 13$ TeV*, Tech. Rep. (CERN, Geneva, 2023).
- [58] *Search for diphoton resonances in the 66 to 110 GeV mass range using 140 fb^{-1} of 13 TeV pp collisions collected with the ATLAS detector*, Tech. Rep. (CERN, Geneva, 2023) all figures including auxiliary figures are available at <https://atlas.web.cern.ch/Atlas/GROUPS/PHYSICS/CONFNOTES/ATLAS-CONF-2023-035>.

- [59] A. Tumasyan *et al.* (CMS), Searches for additional Higgs bosons and for vector leptoquarks in $\tau\tau$ final states in proton-proton collisions at $\sqrt{s} = 13$ TeV, *JHEP* **07**, 073, [arXiv:2208.02717 \[hep-ex\]](#).
- [60] J. Cao, X. Guo, Y. He, P. Wu, and Y. Zhang, Diphoton signal of the light higgs boson in natural nmssm, *Physical Review D* **95**, [10.1103/physrevd.95.116001](#) (2017).
- [61] T. Biekötter, S. Heinemeyer, and G. Weiglein, 95.4 gev diphoton excess at atlas and cms, *Phys. Rev. D* **109**, 035005 (2024).
- [62] T. Biekötter, S. Heinemeyer, and G. Weiglein, The cms di-photon excess at 95 gev in view of the lhc run 2 results, *Physics Letters B* **846**, 138217 (2023).
- [63] A. Arhrib, R. Benbrik, and S. Moretti, Bosonic Decays of Charged Higgs Bosons in a 2HDM Type-I, *Eur. Phys. J. C* **77**, 621 (2017), [arXiv:1607.02402 \[hep-ph\]](#).
- [64] A. Arhrib, R. Benbrik, R. Enberg, W. Klemm, S. Moretti, and S. Munir, Identifying a light charged Higgs boson at the LHC Run II, *Phys. Lett. B* **774**, 591 (2017), [arXiv:1706.01964 \[hep-ph\]](#).
- [65] A. Arhrib, R. Benbrik, S. Moretti, A. Rouchad, Q.-S. Yan, and X. Zhang, Multi-photon production in the Type-I 2HDM, *JHEP* **07**, 007, [arXiv:1712.05332 \[hep-ph\]](#).
- [66] A. Arhrib, R. Benbrik, H. Harouiz, S. Moretti, Y. Wang, and Q.-S. Yan, Implications of a light charged Higgs boson at the LHC run III in the 2HDM, *Phys. Rev. D* **102**, 115040 (2020), [arXiv:2003.11108 \[hep-ph\]](#).
- [67] A. Arhrib, R. Benbrik, M. Krab, B. Manaut, S. Moretti, Y. Wang, and Q.-S. Yan, New discovery modes for a light charged Higgs boson at the LHC, *JHEP* **10**, 073, [arXiv:2106.13656 \[hep-ph\]](#).
- [68] Y. Wang, A. Arhrib, R. Benbrik, M. Krab, B. Manaut, S. Moretti, and Q.-S. Yan, Analysis of $W^\pm + 4\gamma$ in the 2HDM Type-I at the LHC, *JHEP* **12**, 021, [arXiv:2107.01451 \[hep-ph\]](#).
- [69] A. Arhrib, R. Benbrik, M. Krab, B. Manaut, S. Moretti, Y. Wang, and Q.-S. Yan, New Light H^\pm Discovery Channels at the LHC, *Symmetry* **13**, 2319 (2021), [arXiv:2110.04823 \[hep-ph\]](#).
- [70] Z. Li, A. Arhrib, R. Benbrik, M. Krab, B. Manaut, S. Moretti, Y. Wang, and Q. S. Yan, Discovering a light charged Higgs boson via $W^{\pm*} + 4b$ final states at the LHC, (2023), [arXiv:2305.05788 \[hep-ph\]](#).